Supporting Information

d'Ovidio et al. 10.1073/pnas.1004620107

SI Text

Validation of PHYSAT Data at the Confluence of Malvinas and Brazil's Currents. The PHYSAT algorithm has been already validated at the global scale (1, 2). Here we discuss the consistency of PHYSAT observations with regional data at the Malvinas and Brazil's currents confluence.

The background presence of nanoeukaryotes detected by the PHYASAT algorithm in the region of our study is indeed expected due to the ubiquitous presence of these organisms in oligotrophic conditions like before and after the blooming season and in the subtropical gyre.

Regarding the more complex spatial community structures detected by PHYSAT in the region, most of previously available information is concentrated along the shelf break. Along this marginal region, coccolithophorids have been often considered responsible for the blue spectroscopic signature of the strong chlorophyll concentration during spring and summer (3) and recurrently detected by PHYSAT as well (Fig. 2*B* and Figs. S2–S5). More recently, the Patagonia experiment (PATEX) campaigns have allowed us to construct a more detailed picture of the phytoplanktonic dynamics and communities in this region.

The bloom along the shelf break has been described as an early-spring, diatom-dominated bloom initiated by the shoaling of the mixed layer of the nutrient-rich Malvinas waters, followed by coccolithophorids when oligotrophic conditions set in (4). This diatom-to-coccolithophorid succession along the shelf break is also a recurrent observation in PHYSAT data, found in all the years of our analysis. The first PATEX campaign occurred in October–November 2004 and is reported in ref. 5. A high resolution, daily pixel-to-station match up between PATEX stations and PHYSAT is not possible, either because of the large cloud cover (very frequent in this area) or because some stations have been positioned in very high chlorophyll (out of the operating range of the PHYSAT algorithm), or because no type were dominant when the satellite has made its measurements. However, along the shelf break, PHYSAT indicates for early November 2004 a transitional region between a diatom-dominated and a nanoeukariote-dominated patch (Fig. S7, *Left*). The presence of this region agrees with PATEX data, which consists of a phytoplankton assemblage dominated by diatoms (80%, cell number) and nanoflagellate (20%) (figure 7 in ref. 5). In contrast with the 2002 case described in our analysis, during the November 2004 no coccolithophorid-dominated bloom was detected along the shelf break neither in PATEX, nor in PHYSAT (Fig. S7, *Left*). During PATEX, the presence of small-size coccolithophorids was interpreted as the inoculum of a subsequent bloom dominated by this type (ref. 6, p. 1164), again matching PHYSAT data, which detects a coccolithophorids bloom in December 2004 (Fig. S7, *Right*).

Synechococcus blooms (appearing as a few scattered points in all PHYSAT images, with the exception of the mesoscale patch of Fig. S3) have not been reported in the Patagonian shelf break during PATEX cruises. However, significative presence of *Synechococcus* has been detected in association with diatoms in the convergence zone between 40°S and 50°S during the Atlantic Meridional Transect (7).

The PHYSAT algorithm can single out *Phaeocystis* in a nanoeukariote bloom when they form agglomerates because of the optical properties of the white mucus exuded by cells. The detection of *Phaeocystis* agglomerate in some of the images that we analyzed is consistent with the observation that the most abundant nanoeukariotes found in PATEX was indeed *Phaeocystis* (figure 8 in ref. 5).

1. Alvain S, Moulin C, Dandonneau Y, Bréon FM (2005) Remote sensing of phytoplankton groups in case 1 waters from global SeaWiFS imagery. *Deep-Sea Res Pt I* 52:1989–2004.
2. Alvain S, Moulin C, Dandonneau Y, Loisel H (2008) Seasonal distribution and succession of dominant phytoplankton groups in the global ocean: A satellite view. *Global Biogeochem Cy* 22:GB3001.
3. Brown CW, Podestà GP (1997) Remote sensing of coccolithophore blooms in the western south Atlantic ocean. *Remote Sens Environ* 60:83–91.
4. Signorini SR, et al. (2006) Seasonal and interannual variability of calcite in the vicinity of the Patagonian shelf break (38°S–52°S). *Geophys Res Lett* 33:L16610.
5. Garcia VC, et al. (2008) Environmental factors controlling the phytoplantkon blooms at the Patagonia shelf-break in spring. *Deep-Sea Res Pt I* 55:1150–1166.
6. Garcia CAE, Sarma YVB, Mata MM, Garcia VMT (2004) Chlorophyll variability and eddies in the Brazil-Malvinas confluence region. *Deep-Sea Res Pt II* 51:159–172.
7. Zubkov MV, Sleigh MA, Burkill PH, Leakey RJG (2000) Picoplankton community structure on the Atlantic Meridional Transect: A comparison between seasons. *Prog Oceanogr* 45:369–386.

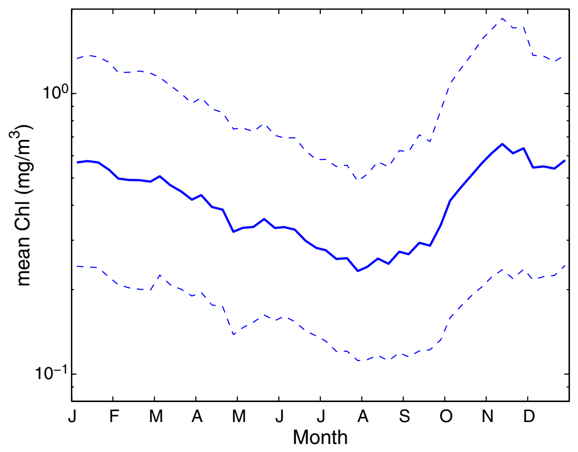

Fig. S1. Time series of mean Chl concentration (log values) from Sea-Viewing Wide Field-of-View Sensor (SeaWiFS) images in the region of Fig. 2 *D–F*. The bloom starts in August and reaches its climax in November. Note the large standard deviation, indication of the strong Chl variability in the region and of the non-Gaussian shape of the Chl distribution (see Fig. S6).

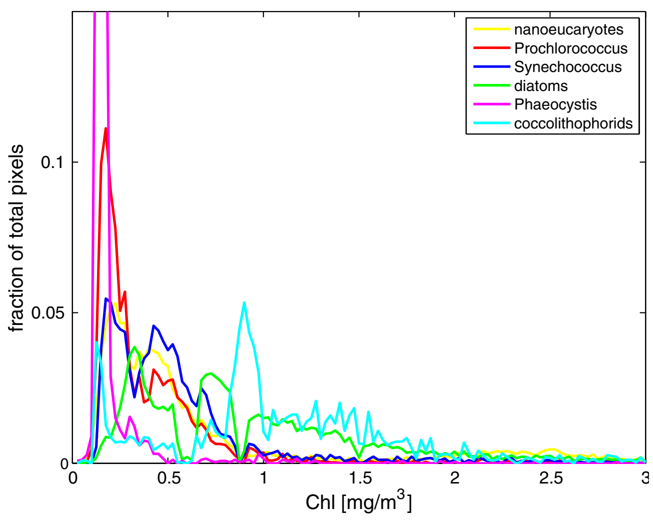

Fig. S2. By-group chlorophyll distributions for November and December 2001 in the region displayed in Fig. 2 *C–F*. The distributions overlap substantially (even if, as expected, maxima and averages of chlorophyll concentration can differ from group to group).

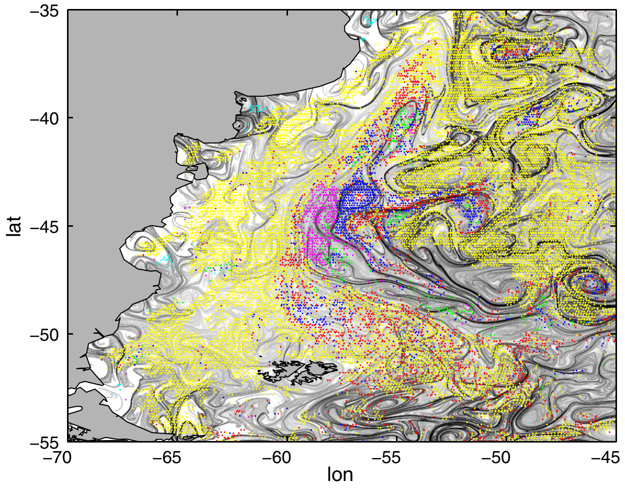

Fig. S3. Maps of dominant planktonic types derived by reprocessing ocean color images (SeaWiFS) by the PHYSAT algorithm (color codes as in Fig. 1) off Patagonia on October 15, 2000. Confluence regions show typically a plankton community with (sub-)mesoscale filamentary spatial structure. Such structures compare well with the transport barriers (superimposed in black) derived by Lagrangian reanalysis of altimetry-derived surface velocities.

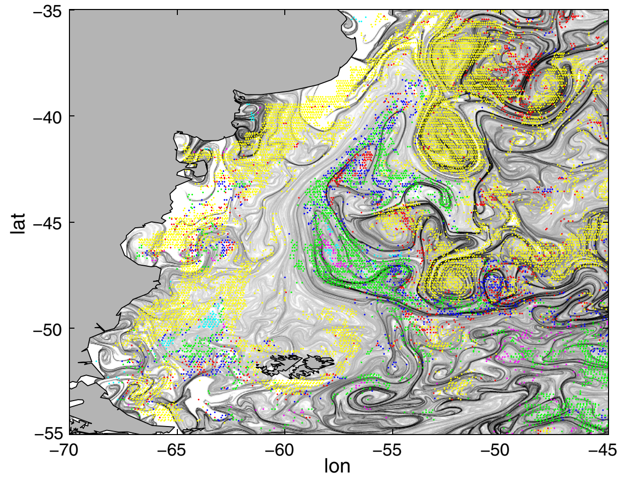

Fig. S4. Maps of dominant planktonic types with superimposed altimetry-derived transport barriers (color codes as in Fig. 1) off Patagonia on December 10, 2000. See comment of Fig. S3.

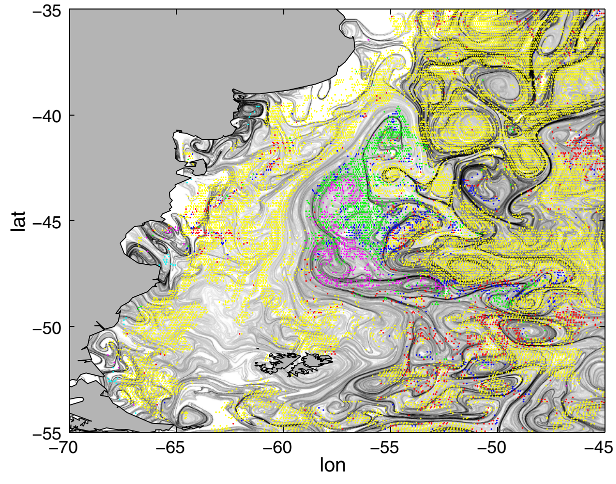

Fig. S5. Maps of dominant planktonic types with superimposed altimetry-derived transport barriers (color codes as in Fig. 1) off Patagonia on October 1, 2002. See comment of Fig. S3.

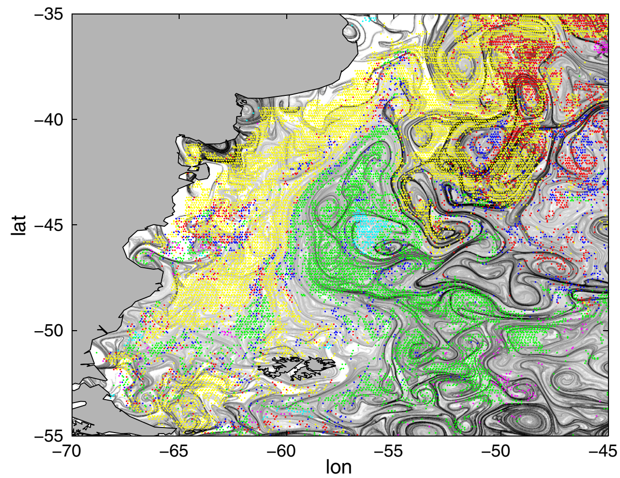

Fig. S6. Maps of dominant planktonic types with superimposed altimetry-derived transport barriers (color codes as in Fig. 1) off Patagonia on December 24, 2002. See comment of Fig. S3.

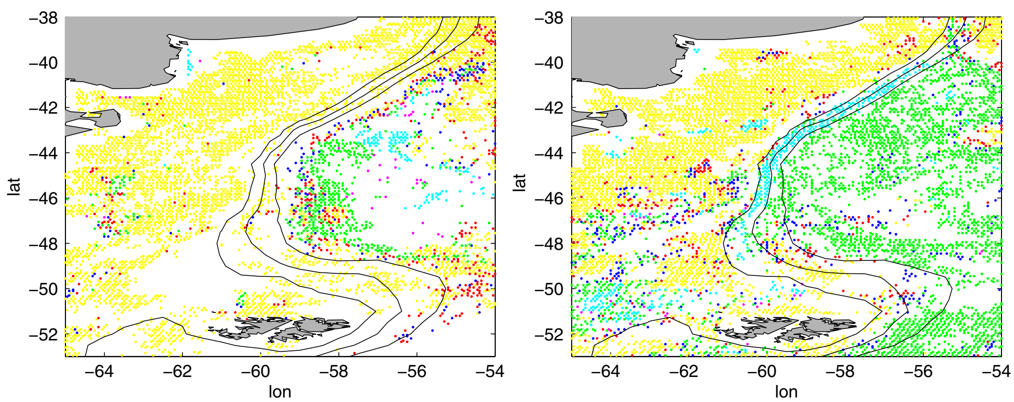

Fig. S7. Maps of dominant planktonic types during PATEX I campaign (November 1–8, 2004, *Left*) and 1 mo after (December 1–8, 2004). The −1000, −500, −200 bathymetry lines have been overimposed for comparison with the figures in Garcia et al. 2008 (5).

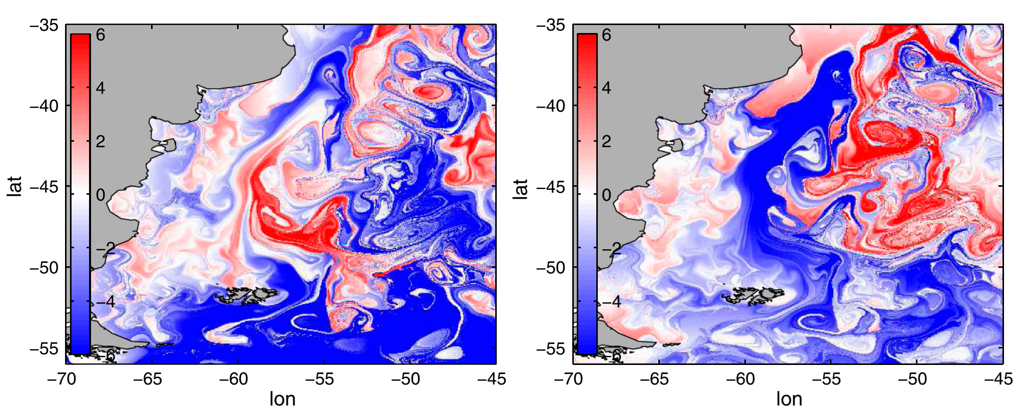

Fig. S8. Longitudinal (*Left*) and latitudinal (*Right*) displacement in degrees of water parcels in a 3-mo backward-in-time advection experiment based on altimetry-derived velocities.

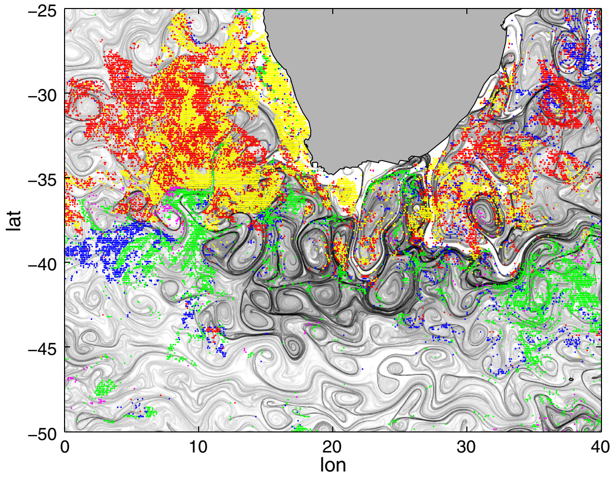

Fig. S9. Maps of dominant planktonic types with superimposed altimetry-derived transport barriers (color codes as in Fig. 1) at the confluence of the Antarctic Circumpolar and Aguilhas currents on January 3, 2001. See comment of Fig. S3.

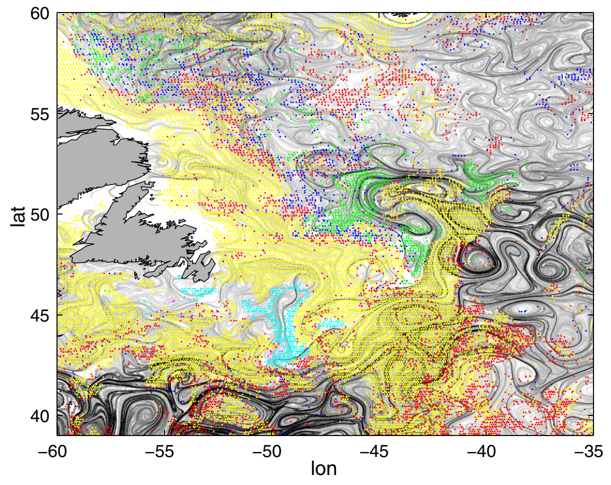

Fig. S10. Maps of dominant planktonic types with superimposed altimetry-derived transport barriers (color codes as in Fig. 1) at the confluence of the Labrador and North Atlantic currents, July 19, 2000.